Investigation of the influence of divertor recycling on global plasma confinement in JET

P. Tamain[a*], E. Joffrin[a], H. Bufferand[a], A. Järvinen[b], S. Brezinsek[c], G. Ciraolo[a], C. Giroud[d], E. Delabie[e], L. Frassineti[f], M. Groth[b], B. Lipschutz[g], S. Marsen[h] , P. Lomas[d], S. Menmuir[f], M. Oberkofler[i], M. Stamp[d], S. Wiesen[c] and JET EFDA contributors[1]

JET-EFDA, Culham Science Centre, Abingdon, OX14 3DB, UK

[a] *CEA, IRFM, F-13108 Saint-Paul-lez-Durance, France*

[b] *Aalto University, Espoo, Finland.*

[c] *Institut für Energie- und Klimaforschung IEK-4, FZJ., TEC, 52425 Jülich, Germany*

[d] *Culham Centre for Fusion Energy, OX14 3DB, Abingdon, United Kingdom*

[e] *FOM Institute for Plasma Physics Rijnhuizen, Postbus 1207, 3430 BE Nieuwegein, The Netherlands*

[f] *Royal Institute of Technology KTH, SE-10691 Stockholm, Sweden*

[g] *Department of Physics, University of York, Heslington, York YO10 5DD, UK*

[h] *Max-Planck-Institut for Plasma Physics, Greifswald, Germany*

[i] *Max-Planck-Institut für Plasmaphysik, 85748 Garching, Germany*

Abstract

The impact of the divertor geometry on the global plasma confinement in type I ELMy H-mode has been investigated in the JET tokamak. Discharges have been performed in which the position of the strike-points was changed while keeping the bulk plasma's equilibrium essentially unchanged. Large variations of the global plasma confinement have been observed, the H_{98} factor changing from typically 0.7 when the outer strike-point is on the vertical target to 0.9 when it is located in the pump duct entrance. Profiles are mainly impacted in the pedestal but core profiles' peaking is also modified. Although substantial differences are observed in the divertor conditions, none seem to correlate directly with the confinement. Modelling with the EDGE2D-EIRENE and SOLEDGE2D-EIRENE transport

codes exhibits differences in the energy losses due to neutrals inside the separatrix, but orders of magnitude are too low to explain simply the impact on the confinement.

PSI-21 keywords: Divertor modelling, Divertor geometry, Energy confinement, JET, Neutrals

PACS: 52.55.Fa, 52.55.Rk, 52.65.-y

**Corresponding author address:* CEA, IRFM, F-13108 Saint-Paul-lez-Durance, France.

**Corresponding author E-mail:* patrick.tamain@cea.fr

Presenting author: Dr Patrick Tamain

Presenting author e-mail: patrick.tamain@cea.fr

[1] *(See App. of F.Romanelli et al., Proc. of the 24th IAEA Fusion Energy Conf. 2012, San Diego, USA)*

1 Introduction

The reduction of the global plasma confinement observed in the JET base line scenario (type I ELMy H-mode) since the installation of the ITER-Like Wall has highlighted the importance of the edge plasma and plasma-wall interaction physics in determining the performances of a reactor [1]. It is not clear yet whether this effect is predominantly related to the change in the impurity mix or in the recycling pattern of the main specie, either in the divertor or in the main chamber, and whether the impact is direct or due to changes in the pedestal stability [2]. However, the importance of the particle source as a key control parameter is confirmed by the degradation of the confinement obtained when puffing deuterium in order to limit impurity accumulation in the plasma [3]. As the main particles input to the plasma, recycling is hence likely to play a role in the physics of confinement. Moreover, the change of the divertor material from carbon to tungsten has changed the recycling properties of the divertor. In particular, it is expected that neutrals recycle from the wall with more energy for a tungsten target than for a carbon one. The distribution of molecules and atoms is also likely to change significantly [4], resulting in different particle and energy sources and sinks distribution in the edge plasma.

In this work, we investigate the possible influence of divertor recycling on the plasma confinement in type I ELMy H-mode, based on the analysis and modelling of dedicated experiments conducted in JET. Series of plasmas were performed in which the divertor configuration was changed while keeping the geometry of the main plasma as well as external actuators (fuelling, heating power) as constant as possible. The paper is constructed along the following outline: the experimental strategy is described in section 2; main results concerning the influence of the divertor geometry on the confinement are presented in section 3; section 4 details the measured changes in divertor recycling conditions; first results of modelling with edge transport codes are reported in section 5; finally, discussion and conclusions are presented in section 6.

2 Experimental strategy

The data used in this paper are based on a series of type ELMy H-mode discharges run in JET. In order to isolate the effect of divertor recycling, 3 different configurations were tested in which the geometry of the divertor was varied by moving the position of the strike-points with respect to the pump duct entrances. Low triangularity plasmas were considered in order to minimize the influence of main chamber recycling. Figure 1 shows the resulting magnetic equilibria as reconstructed by EFIT [5]. Owing to the position of the outer strike-point, the 3 cases will be referred to as the horizontal, corner and vertical target cases in the remainder of the paper. Note that the hereby vertical target case should not be confused with what is usually referred to as the vertical targets configuration in JET, in which both the inner and outer strike-points lie on the vertical targets. These equilibria were designed in order to keep the impact of the changes in the divertor on the magnetic equilibrium of the bulk plasma minimal. Table 1 gives an overview of their main geometrical characteristics.

Plasmas were run at a plasma current of 2.5MA. Scans in deuterium fuelling rate were performed, the gas being puffed from the inner private flux region in most cases, although a few shots were run with gas puff from the main chamber in the outboard mid-plane. Two heating power levels were used intra-shot: $P_{NBI} \approx 14 \pm 2MW$ and $P_{NBI} \approx 22 \pm 2MW$. Time traces of 3 typical discharges, one for each configuration, are plotted in Figure 2.

3 Impact on confinement and profiles

The time evolution of the H_{98} confinement factor [6] is also shown in Figure 2. At equal fuelling rates and heating powers, the discharges run in the horizontal and the vertical target configurations have similar confinement of the order of 0.7, while the corner configuration exhibits a confinement factor peaking above 0.9 in the 23MW heating phase. This trend is

found in all the shots of the database, as plotted in Figure 3. For comparable puffing rates, the plasmas run in corner configuration have H_{98} confinement factors 0.1 to 0.2 larger than the ones run in the horizontal configuration. The vertical configuration is characterized by a large spread between the low power cases and high power cases indicating that the low power cases are probably marginally above the LH power threshold. In each configuration, the deuterium puffing has a negative impact of the confinement, as already reported [3], but the localization of the puff does not seem to be a dominant player.

The changes in the confinement are corroborated by the density, temperature and pressure profiles plotted in Figure 4. The corner case is characterized by pressures substantially higher than the two other cases, the difference reaching 50% at the centre of the plasma. Interestingly, the gain is made either on the temperature or on the density. The horizontal and corner configuration discharges present similar density profiles, but the electron and ion temperatures are 50% larger in the corner case. On the contrary, the vertical configuration discharge exhibits much lower density than the two others, but the electron temperature is similar to that of the corner case and the ion temperature profile is intermediate between the horizontal and corner cases. This suggests that the mechanisms explaining the degradation of the confinement in the horizontal and vertical configurations with respect to the corner one are possibly different. Differences in the profiles are both due to variations in the pedestal (P_e is 50% larger at the top of the pedestal in the corner configuration) and to changes in the core gradients of the quantities.

Finally, let's point out that the changes in the confinement cannot be explained by the variations in the bulk plasma's geometry. Applying the ITER98 scaling law [6] (in which only the elongation appears as an influential shaping parameter) to the figures given in Table **1** would lead to variations of the confinement of the order of 2% between the three configurations. The effect of the triangularity is subject to discussions [7][8][9], but it is unlikely that a variation of 5% would impact significantly the confinement. Finally, the

distance of the separatrix to the main chamber wall does not vary significantly with respect to the Scrape-Off Layer width, excluding a large influence on the confinement.

4 Impact on the divertor conditions

Let us now focus on the edge plasma and divertor conditions. Figure 5 shows the inner and outer divertor D_α radiation as a function of the strike-point position and of the fuelling rate. As expected, the D_α radiation scales up with the fuelling rate. The puff location has little influence on the signal, proving that the divertor particle source is dominated by recycling. A strong dependence is found between the strike-points location and the amplitude of the divertor D_α light emission, with a drop of a factor of 3 at similar puffing rate between the horizontal and the vertical configuration. The corner cases have intermediate inner divertor radiation. For the outer divertor, a similar trend is found, with the difference that a minimum radiation seems to exist for the corner configuration. This could however be due to partial blinding of the spectrometer in the corner configuration so that one cannot conclude on the significance of this minimum.

These observations point towards a reduction of the recycling particle flux when moving the strike-points outward. They are confirmed by the neutral pressure measured in the sub-divertor which increases by 50% when moving from the horizontal to the vertical configuration. Since the pumped particle flux is directly proportional to the sub-divertor pressure, more particles are pumped in the vertical configuration leading to a reduction of the effective recycling coefficient of particles. This conclusion is corroborated by Langmuir probes measurements. Although little data is available due to the absence of probes when the strike-points are located in the corners (outer strike-point in the corner configuration and inner strike point in the vertical configuration), the particle flux reaching the target is about 60% lower (peak and integral value) at the outer-strike point in the vertical configuration compared with the horizontal one. This way, strong evidence of changes in the divertor recycling pattern

is found when comparing the 3 configurations. It remains however hard to correlate these changes with the global confinement, as these do not go through an extremum when the confinement reaches its maximum for the corner configuration.

5 Modelling with EDGE2D and SOLEDGE2D fluid codes

In order to interpret the previous results and try to isolate a possible mechanism, simulations have been run with edge transport codes. Two codes are considered, the EDGE2D-EIRENE package [10] and the SOLEDGE2D-EIRENE code [11]. Simulations are run without impurities and with equal upstream densities in order to focus on primary differences in neutral recycling. Figure 6 shows the amplitude of the energy source/sink due to neutrals for the ion specie obtained for each configuration. One can notice the strong interaction of the plasma with the inner and outer baffles in the horizontal and vertical configurations respectively. In the corner configuration, the interaction between the neutrals and the plasma is relatively more confined in the divertor volume. The proximity of the separatrix with the baffles hence tends to delocalize outside the divertor part of the neutrals – plasma interaction. A direct consequence can be found when looking at the impact of neutrals on the plasma inside the separatrix. As shown in Figure **7**, SOLEDGE2D simulations indicate that total power losses due to neutrals inside the separatrix present a minimum for the corner configuration. This minimum is not found in EDGE2D simulations, which might be due to different detailed geometrical treatment of the divertor and upstream conditions and will require more attention. In any case, the amplitudes of the losses in both codes are in the same ball-park and extremely low compared with the heating power, so that they are unlikely to explain the variations in the confinement without invoking an extremely stiff response from the pedestal.

6 Conclusion

Based on a set of dedicated type-I ELMy H-mode discharges run in JET, a large influence of the divertor magnetic configuration (position of the strike points) on the global confinement has been found in the absence of significant change for the bulk plasma shape. Variations of the order of 20% are found, with higher pedestal pressure and larger core pressure gradients when the outer strike-point is located close to the pumping gauge. Analysis of the recycling pattern of particles demonstrates large variations between the tested configurations, but no direct correlation can be inferred. 2D transport modelling suggests that the pedestal – neutrals interactions is reduced for plasmas in which the largest confinement is found, mainly due to a larger distance between the separatrix and the divertor baffles. However, the small amplitude of the perturbation with respect to the total heating power makes it an unlikely explanation for the observed variations. Although the underlying physics remain unidentified, these results indicate the existence of missing parameters in the ITER98 energy confinement time scaling law.

Acknowledgements

This work, supported by the European Communities under the contract of Association between EURATOM and CEA, was carried out within the framework of the European Fusion Development Agreement. The views and opinions expressed herein do not necessarily reflect those of the European Commission. Computations have been performed at the Mésocentre d'Aix-Marseille Université.

References

[1] M. Beurskens *et al.*, Nucl. Fusion **54**, 043001 (2014).

[2] M. Beurskens *et al.*, Plasma Phys. Control. Fusion **55**, 124043 (2013).

[3] E. Joffrin *et al.*, Nucl. Fusion **54**, 013011 (2014).

[4] A. Järvinen, this conference.

[5] L. Lao *et al.*, Nucl. Fusion **25**, 1611 (1985).

[6] ITER Physics Basis, Nucl. Fus. **39**, 2175 (1999).

[7] D.C. McDonald, EFDA JET report **CP(00)03/08** (2000).

[8] G. Saibene *et al*; Nucl. Fus. **39**, 1133 (1999).

[9] G. Saibene *et al.*, Plasma Phys. Control. Fusion **44**, 1769–1799 (2002).

[10] M. Groth *et al.*, Nucl. Fusion **53**, 093016 (2013).

[11] H. Bufferand *et al.*, J. Nucl. Mater. **438**, S445 (2013).

Figures and tables captions

Figure 1: magnetic equilibria of the 3 plasma configurations used in the considered experiment.

Figure 2: time traces of the gas puffing rate, the NBI power, the line-integrated density, the divertor Be radiation ("ELM signal") and H98 confinement factor for three discharges run in each of the three divertor configurations considered in the experiment.

Figure 3: H98 confinement factor as a function of the outer strike-point position. Empty symbols represent discharges at $\boldsymbol{P_{NBI} \approx 14 \pm 2MW}$, full symbols to $\boldsymbol{P_{NBI} \approx 22 \pm 2MW}$. The color scale corresponds to the deuterium fuelling rate. Circles are for plasmas fuelled from the divertor, squares for mid-plane fuelling.

Figure 4: Profiles of main plasma quantities for three discharges, one in each configuration (horizontal - #84772, corner - #84771, vertical - #84773), time-averaged during the high power phase ($\boldsymbol{P_{NBI} \approx 22 \pm 2MW}$). Electron density, temperature and pressure were obtained with the High Resolution Thomson Scattering; ion temperature was measured by charge exchange spectroscopy.

Figure 5: Total Dα radiation from inner and outer divertor as a function of the outer strike-point position. The meaning of symbols and colors is the same as in Figure 3.

Figure 6: Amplitude of energy sources / sinks in the divertor as simulated by SOLEDGE2D in the 3 considered magnetic configuration (log10 scale, in W.m-3) at PNBI=23MW. The dashed pink line is the separatrix.

Figure 7: Energy losses for ions (red full) and electrons (blue empty) due to neutrals inside the separatrix as found in SOLEDGE2D (squares) and EDGE2D (circles) simulations for each of the considered configurations for the high power case.

Table 1: main characteristics of the magnetic equilibria for the 3 considered divertor configurations; lower triangularity, upper triangularity, elongation, q95, Radial Inner Gap (minimal distance to the wall on the inner side) and Radial Outer Gap (same on the outer side).

Figures and tables

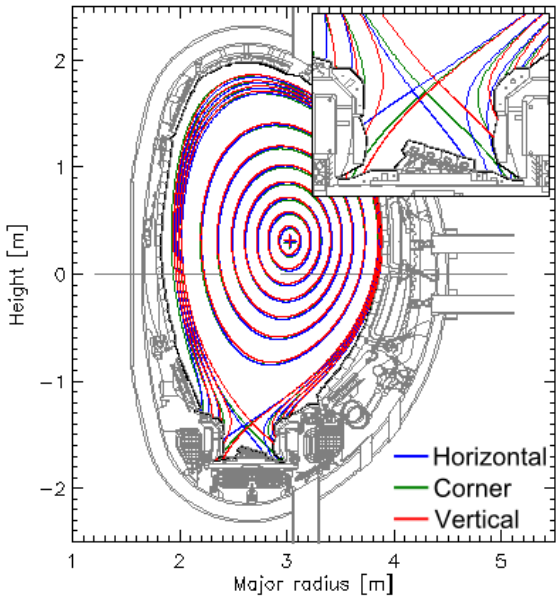

Figure 1: magnetic equilibria of the 3 plasma configurations used in the considered experiment. The upper left box is a zoom on the divertor.

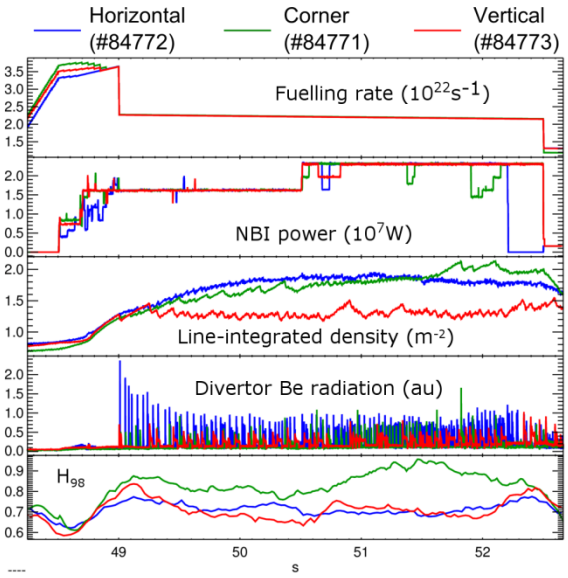

Figure 2: time traces of the gas puffing rate, the NBI power, the line-integrated density, the divertor Be radiation ("ELM signal") and H_{98} confinement factor for three discharges run in each of the three divertor configurations considered in the experiment.

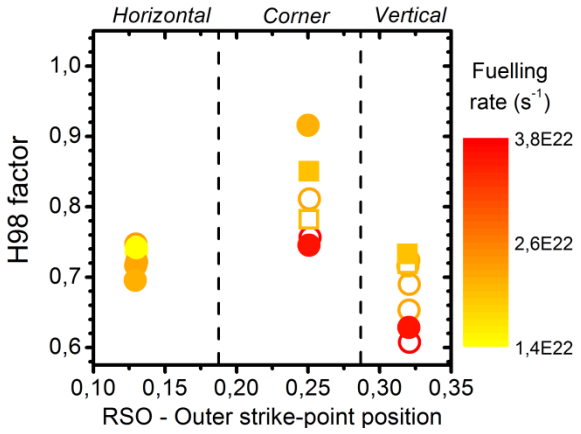

Figure 3: H_{98} confinement factor as a function of the outer strike-point position. Empty symbols represent discharges at $\boldsymbol{P_{NBI} \approx 14 \pm 2MW}$, full symbols to $\boldsymbol{P_{NBI} \approx 22 \pm 2MW}$. The color scale corresponds to the deuterium fuelling rate. Circles are for plasmas fuelled from the divertor, squares for mid-plane fuelling.

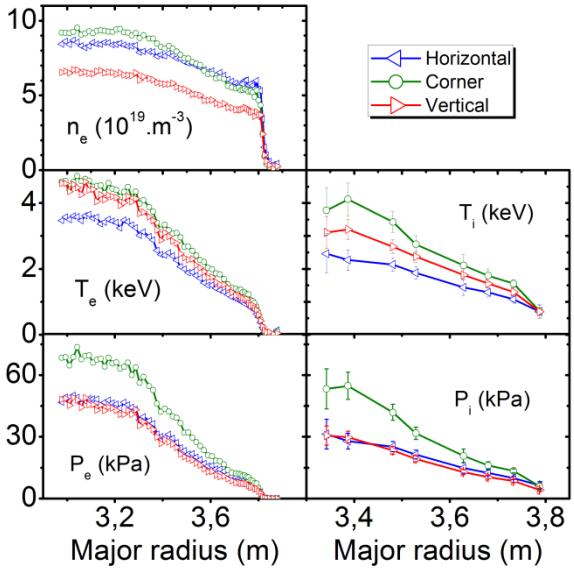

Figure 4: Profiles of main plasma quantities for three discharges, one in each configuration (horizontal - #84772, corner - #84771, vertical - #84773), time-averaged during the high power phase ($\boldsymbol{P_{NBI} \approx 22 \pm 2MW}$). Electron density, temperature and pressure were obtained with the High Resolution Thomson Scattering; ion temperature was measured by charge exchange spectroscopy.

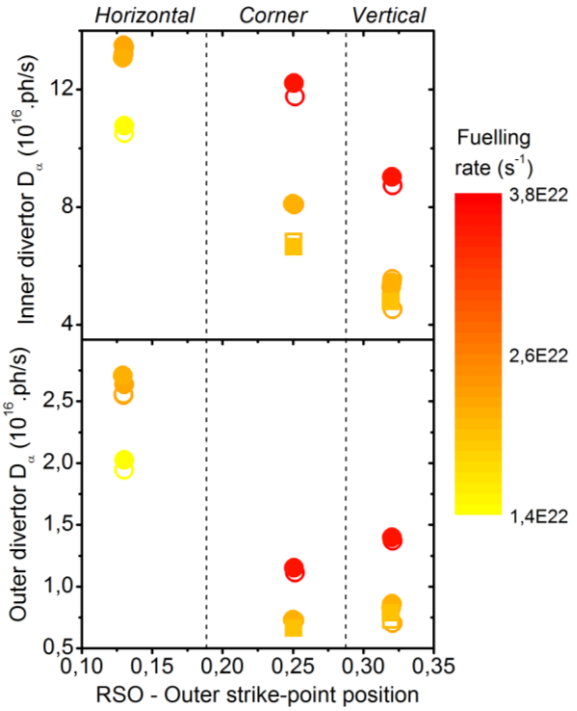

Figure 5: Total D_α radiation from inner and outer divertor as a function of the outer strike-point position. The meaning of symbols and colors is the same as in Figure 3.

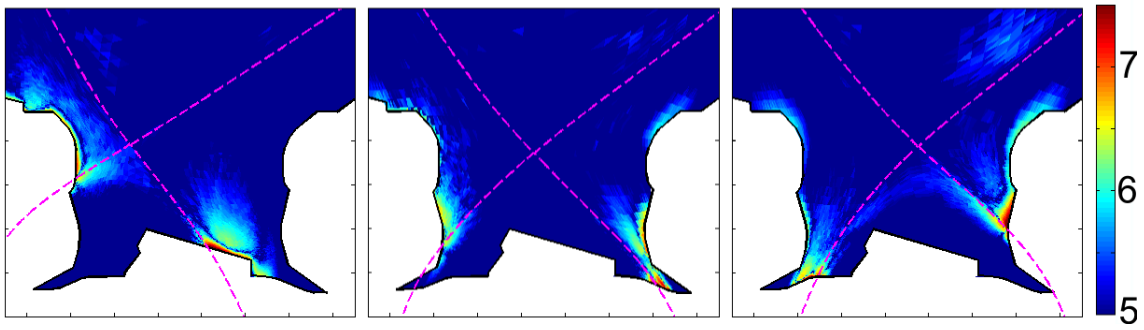

Figure 6: Amplitude of energy sources / sinks in the divertor as simulated by SOLEDGE2D in the 3 considered magnetic configuration (log_{10} scale, in W.m^{-3}) at P_{NBI}=23MW. The dashed pink line is the separatrix.

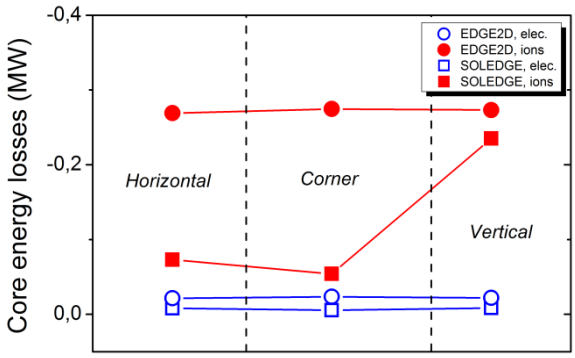

Figure 7: Energy losses for ions (red full) and electrons (blue empty) due to neutrals inside the separatrix as found in SOLEDGE2D (squares) and EDGE2D (circles) simulations for each of the considered configurations for the high power case.

	Lower tri.	Upper tri.	Elongation	q_{95}	RIG	ROG
Horizontal	0.38	0.16	3.2	1.7	19 cm	5.5 cm
Corner	0.32	0.18	3.3	1.7	17 cm	5.5 cm
Vertical	0.28	0.17	3.2	1.7	19 cm	5.5 cm

Table 1: main characteristics of the magnetic equilibria for the 3 considered divertor configurations; lower triangularity, upper triangularity, elongation, q_{95}, Radial Inner Gap (minimal distance to the wall on the inner side) and Radial Outer Gap (same on the outer side).